

Computation of Mistuning Effects on Cascade Flutter

Mani Sadeghi* and Feng Liu†
University of California, Irvine, Irvine, California 92697-3975

A computational method is described for predicting flutter of turbomachinery cascades with mistuned blades. The method solves the unsteady Euler/Navier-Stokes equations for multiple-blade passages on a parallel computer using the message passing interface. A second-order implicit scheme with dual time-stepping and multigrid is used. Each individual blade is capable of moving with its own independent frequency and phase angle, thus modeling a cascade with mistuned blades. Flutter predictions are performed through the energy method. Both phase-angle and frequency mistuning are studied. It is found that phase-angle mistuning has little effect on stability, whereas frequency mistuning significantly changes the aerodynamic damping. The important effect of frequency mistuning is to average out the aerodynamic damping of the tuned blade row over the whole range of interblade phase angles (IBPA). If a tuned blade row is stable over most of the IBPA range, the blades can be stabilized for the complete IBPA range through appropriate frequency mistuning.

Nomenclature

C_h	= coefficient of aerodynamic force in h direction
C_w	= aerodynamic work coefficient
c	= blade chord length
E	= total energy per unit mass
h	= translational blade displacement
p	= static pressure
T	= flutter period
t	= time
u, v	= flow velocity components in x and y directions
u_b, v_b	= grid velocity components in x and y directions
\bar{u}, \bar{v}	= relative velocity components ($u - u_b, v - v_b$)
α	= rotational blade displacement
θ	= stream tube thickness ratio in x direction
Ξ	= flutter damping coefficient
ρ	= density
σ	= interblade phase angle
ω	= flutter frequency

I. Introduction

TURBOMACHINERY designers are striving for increased loading and reduced size and weight of compressor and turbine blade rows, particularly for aircraft engines. As such, the flutter of the turbomachinery blades may become a limiting factor in the design and performance of gas turbine engines. Accurate theoretical and computational methods in predicting the flutter boundary will enable us to achieve high performance and low cost by allowing adequate but not excessive design margins.

Flutter calculations for turbomachinery blade rows often employ Lane's¹ traveling wave model in which the adjacent blades in a blade row are assumed to vibrate at the same frequency but with a constant phase difference, called interblade phase angle (IBPA). With this model, aerodynamic responses of the blade row can be determined by using a single blade passage to minimize the computational effort. Consequently, a phase-shifted periodic boundary condition has to be applied when the IBPA is not zero. The use of the phase-shifted boundary condition and its implementation in a flow code, using the traditional "direct store" method of Erdos and Alzner,² implies that the solution is both temporally and spatially periodic. In an actual machine, blades are never exactly identical

because of manufacturing imperfections, which result in nonidentical vibration frequencies and phase shifts (mistuning) of the blades in a blade row. There is also evidence to show that certain intentional mistuning may improve the flutter characteristics of a blade row.

Kaza and Kielb³ studied effects of mistuning for a cascade oscillating in a coupled bending torsion or uncoupled torsion mode. Aerodynamic loads were calculated on the basis of a linearized incompressible flow method for flat plates. They found that mistuning and alternate mistuning, as well as random mistuning, have a strong beneficial effect in the case of self-excited vibration. The flutter speed was increased by increasing the mistuning level. Crawley and Hall⁴ developed an inverse design procedure for the optimum mistuning of a high-bypass ratio fan. A linearized supersonic aerodynamic theory is used to compute the unsteady forces in the influence coefficient form. Imregun and Ewins⁵ performed numerical studies on a cascade of flat plates in the incompressible subsonic and supersonic Mach number range. The structural behavior was modeled with a lumped-parameter presentation of rigid blade profiles, allowing for structural coupling between the blades. Mistuning and alternate mistuning in particular were found to have positive effects by stabilizing critical vibration modes at the expense of damped ones. A recent experimental and numerical investigation on an annular turbine cascade was done by Nowinski and Panovsky.⁶ The blades were oscillated in a harmonic torsional mode. Three vibrational modes of the blades were tested: the traveling wave mode, the single blade mode, and the alternating blade mode. In the latter test mode, only alternate blades in the cascade were excited in a traveling wave pattern, whereas others remained stationary to simulate frequency mistuning. Nowinski and Panovsky found that alternate frequency mistuning reduced the dependence of the aerodynamic damping coefficient on the IBPA and significantly enhanced the stability of the tested low-pressure turbine cascade.

Except for Nowinski and Panovsky,⁶ all of these authors performed the analysis in the frequency domain by solving an eigenvalue problem of the structural flutter equations with aerodynamic loads as input in the form of influence coefficients. In this paper we propose to study mistuning in the time domain by directly solving the unsteady flow of a cascade under mistuned oscillations. Stability is determined by calculating the aerodynamic damping coefficient as defined in Bölc and Fransson.⁷ Although the method is limited to high mass ratio blades, it provides useful insights into the flutter mechanism, in view of the aerodynamics of the flow through a cascade that undergoes mistuned blade motions. To perform such studies, the flow is no longer considered to be periodic in either space or time. Therefore, the traditional method with phase-shifted boundary conditions cannot be used. Computation for such flows must be done over multiple passages.

In a previous work by Ji and Liu,⁸ a multigrid, time-accurate Navier-Stokes code with a two-equation $k-\omega$ turbulence model was developed to calculate quasi-three-dimensional unsteady flows

Received 8 November 1999; revision received 9 May 2000; accepted for publication 9 May 2000. Copyright © 2000 by Mani Sadeghi and Feng Liu. Published by the American Institute of Aeronautics and Astronautics, Inc., with permission.

*Graduate Researcher, Department of Mechanical and Aerospace Engineering, Student Member AIAA.

†Associate Professor, Department of Mechanical and Aerospace Engineering, Member AIAA.

around multiple oscillating turbine blades. The code was made parallel by using the message passing interface (MPI), such that multiple passages could be calculated without the use of phase-shifted periodic boundary conditions for blade flutter problems. The code ran efficiently on regular parallel computers or networked clusters of workstations or PCs. In this paper, we extend the method by Ji and Liu to studies of mistuning effects. The standard configuration 4 of a turbine cascade compiled by Böös and Fransson⁷ is used as a test case. Damping coefficients are obtained for various IBPAs for the tuned case and compared with results for both phase-angle mistuning and frequency mistuning. It is found that for this case, mistuning of phase shift has small effects on the flutter characteristics, whereas mistuning of frequency has a significant effect on the damping coefficients of each blade in the row. Frequency mistuning has the effect of averaging out the damping coefficient for the tuned blade row over the whole range of IBPA because of a temporally changing phase difference between each blade and the adjacent blade. Therefore, if a tuned blade row is stable for a majority of the IBPA range, alternate and random frequency mistuning can stabilize the blades over the complete range of IBPA. In fact, random frequency mistuning eliminates the dependence of the aerodynamic damping coefficient on the IBPA. The effect of the degree of frequency mistuning is also discussed in view of the damping coefficient as a measure for stability.

II. Computational Method

For a two-dimensional control volume V with moving boundary ∂V the quasi three-dimensional Favre-averaged Navier–Stokes equations with a k – ω turbulence model can be written as follows:

$$\begin{aligned} \frac{\partial}{\partial t} \iint_V \theta(x) \mathbf{w} \, dV + \oint_{\partial V} \theta(x) \mathbf{f} \, dS_x + \theta(x) \mathbf{g} \, dS_y \\ = \oint_{\partial V} \theta(x) \mathbf{f}_\mu \, dS_x + \theta(x) \mathbf{g}_\mu \, dS_y + \iint_V \mathbf{S} \, dV \end{aligned} \quad (1)$$

where the vector

$$\mathbf{w} = \begin{bmatrix} \rho \\ \rho u \\ \rho v \\ \rho E \\ \rho k \\ \rho \omega \end{bmatrix} \quad (2)$$

contains the conservative flow variables plus the turbulent kinetic energy k and the specific dissipation rate ω , in the k – ω turbulence model by Wilcox.⁹ The vectors

$$\mathbf{f} = \begin{bmatrix} \rho \bar{u} \\ \rho u \bar{u} + p \\ \rho v \bar{u} \\ \rho E \bar{u} + \rho u \\ \rho k \bar{u} \\ \rho \omega \bar{u} \end{bmatrix}, \quad \mathbf{g} = \begin{bmatrix} \rho \bar{v} \\ \rho u \bar{v} + p \\ \rho v \bar{v} \\ \rho E \bar{v} + \rho u \\ \rho k \bar{v} \\ \rho \omega \bar{v} \end{bmatrix} \quad (3)$$

are the Euler fluxes with the velocity components \bar{u} and \bar{v} relative to the moving boundary of the control volume. The terms \mathbf{f}_μ and \mathbf{g}_μ are the viscous fluxes in the x and y directions, respectively. The source vector \mathbf{S} includes terms due to the variation of $\theta(x)$, which is defined as the stream tube thickness at each x location divided by the stream tube thickness at $x = 0$. The use of $\theta(x)$ is to account for the cross-sectional area change of the blade passage due to a blade height variation in the flow direction. A detailed description of the terms in Eqs. (1–3) can be found in Ref. 8.

A finite volume method is used for spatial discretization. Equation (1) can then be written in semidiscrete form:

$$\frac{d\mathbf{w}}{dt} + \mathbf{R}(\mathbf{w}) = 0 \quad (4)$$

where \mathbf{R} is the vector of residuals, consisting of the spatially discretized flux balance of Eq. (1). Time accuracy is achieved by using

a second-order implicit time-discretization scheme, which is recast into a pseudotime formulation, as proposed by Jameson¹⁰:

$$\frac{d\mathbf{w}}{dt^*} + \mathbf{R}^*(\mathbf{w}) = 0 \quad (5)$$

For each physical time step in Eq. (4), the solution is sought by solving Eq. (5) for a steady state in pseudotime t^* . The benefit of this reformulation is that convergence acceleration techniques, such as local time stepping, residual smoothing, and a multigrid method, can be used in pseudotime without sacrificing time accuracy.

At the inlet and outlet, the boundary conditions are formulated using the one-dimensional Riemann invariants normal to the boundary. No noticeable reflections from the boundaries were found. A phase-shifted periodic boundary condition is applied at the boundaries between the passages. For tuned blade rows this condition becomes

$$\mathbf{w}_l = \mathbf{w}_u(x, t - \sigma/\omega) \quad (6)$$

where subscripts l and u denote the lower and upper boundaries of a blade passage, σ is the IBPA, and ω is the angular frequency of the blade vibration. To perform calculations with mistuned blades, the conventional direct store method by Erdos and Alzner² used to apply the phase-shifted periodic boundary condition is replaced by pure periodic boundary conditions through the use of multiple passages. The minimum IBPA that can be simulated is related to the number of blade passages used in the computation by the following equation:

$$\sigma(\text{deg}) = \pm \frac{360 \text{ deg}}{\text{number of blade passages}} \quad (7)$$

Although this limits the IBPA to be discrete numbers and large numbers of blade passages have to be computed for small IBPA, it has the advantage of extending the calculations to a full annulus with nonperiodic motions and mistuned blades. The IBPA σ and the oscillation frequency ω can vary from blade to blade, which allows the investigation of both phase-angle mistuning and frequency mistuning.

Figure 1 shows a cylindrical cut of a blade passage. The x coordinate is along the engine axis. The y coordinate is the circumferential coordinate, which is equivalent to $r\theta$ for a cylindrical cut at radius r ; c is the chord length of the blade profile; and c_x is the axial chord. The blades are assumed to be rigid and follow a motion of a combined bending and torsion mode. For the m th blade, the bending and torsion motions can be specified as

$$\mathbf{h}^{(m)}(t) = a(\mu_x \mathbf{e}_x + \mu_y \mathbf{e}_y) \exp[i(\omega_m t + \varphi_m)] \quad (8)$$

$$\alpha^{(m)}(t) = a(\mu_\alpha/c) \exp[i(\omega_m t + \varphi_m)] \quad (9)$$

where α is positive counterclockwise in Fig. 1. If $\mathbf{h}(t)$ is written as

$$\mathbf{h}^{(m)}(t) = h_x^{(m)}(t) \mathbf{e}_x + h_y^{(m)}(t) \mathbf{e}_y \quad (10)$$

we can write

$$\begin{bmatrix} h_x^{(m)}(t) \\ h_y^{(m)}(t) \\ \alpha^{(m)}(t) \end{bmatrix} = a \begin{bmatrix} \mu_x \\ \mu_y \\ \mu_\alpha/c \end{bmatrix} \exp[i(\omega_m t + \varphi_m)]$$

$$m = 0, 1, 2, \dots \quad (11)$$

where m stands for the blade number; $\omega_m = 2\pi f_m$ and φ_m are the angular frequency and the phase of the forced vibration of blade m . In the tuned case, the constant IBPA is $\sigma = \varphi_m - \varphi_{m-1}$. The parameter

$$\mu = \begin{bmatrix} \mu_x \\ \mu_y \\ \mu_\alpha \end{bmatrix} \quad (12)$$

characterizes the specified modal shape of the combined bending and torsion motion; a is a general dimensionless amplitude. The

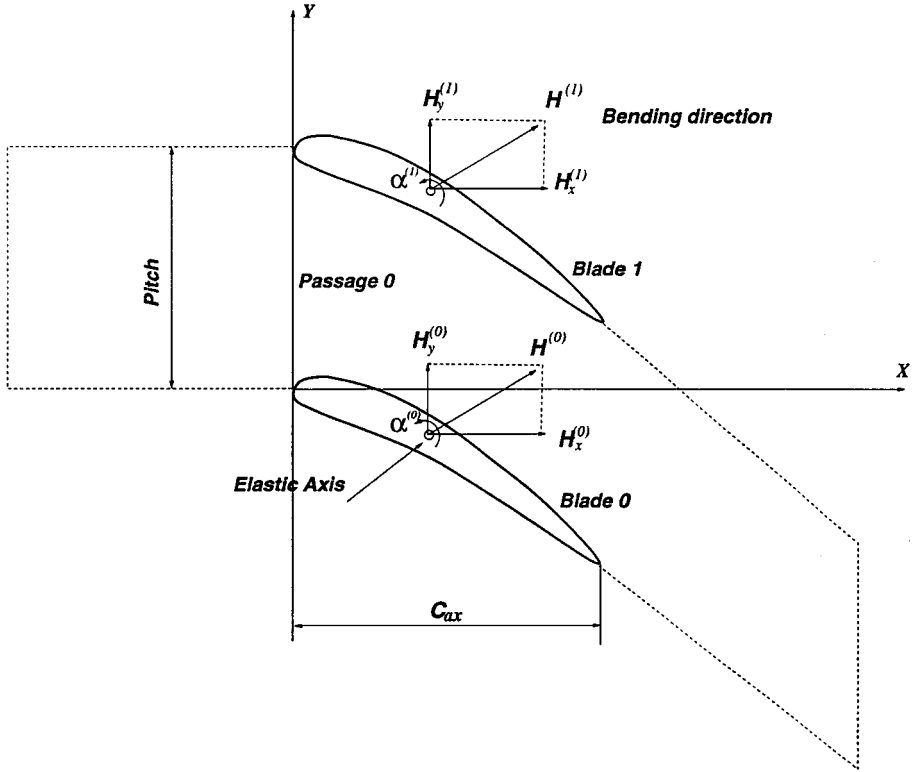


Fig. 1 Blade geometry and motion definition.

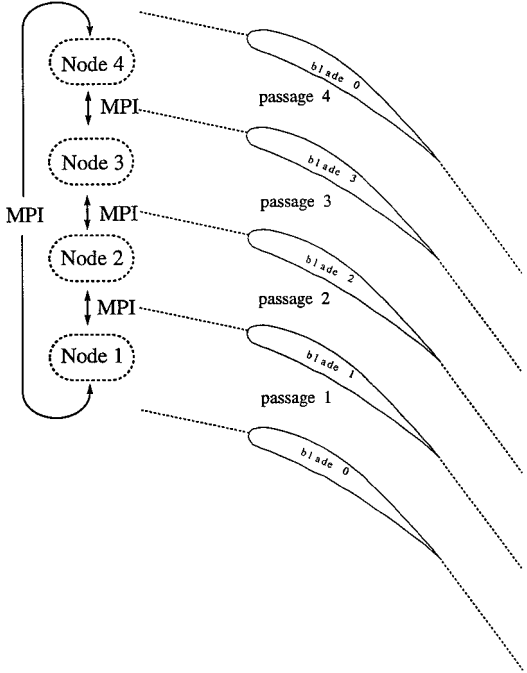


Fig. 2 Multiple-passage computation using MPI.

modal parameters μ_x , μ_y , and μ_α all have the dimension of length. In general, they may be complex numbers when there are phase differences among the x , y bending motions and the torsion motion. However, standard configuration 4 does not include torsional vibration, so that the current work is performed with a pure bending mode, with a bending angle

$$\delta = \tan^{-1}(\mu_y / \mu_x)$$

A parallel algorithm is implemented in which each processor computes the flow through one blade passage, and communication between blade passages is achieved by using MPI (Fig. 2). The

method scales very well on both parallel computers and networked workstations. The accuracy of the numerical method and the efficiency of the parallel implementation have been validated in Ref. 8.

III. Results and Discussion

A. Computation for Tuned Blades

Bölc and Fransson⁷ defined several standard test cases for flutter investigation in turbomachinery. The case 552B of standard configuration 4 with inlet Mach number $M_1 = 0.28$, outlet isentropic Mach number $M_{is,2} = 0.90$ and inlet flow angle $\beta_1 = -45$ deg are chosen for comparison. Earlier comparisons between Euler and Navier-Stokes results (Ref. 8) did not indicate significant viscous effects with this configuration. Therefore, in the current work, only Euler calculations were performed. The calculations were performed on a mesh of 96×24 cells. Calculations on a finer mesh with 112×64 cells did not yield significantly different results. In previous investigations by Liu and Ji,¹¹ a number of 32 real-time steps per flutter period was found to be sufficient to resolve temporal variations. Alonso and Jameson¹² in a separate study of wing flutter found that 36 time steps per period are sufficient. In the current work 64 time steps per period were performed, with each real-time step including 46 pseudotime iterations with a Courant-Friedrichs-Lowy number of 6. The unsteady residual was reduced by three orders of magnitude in each real-time step.

Figure 3 shows the steady-state isentropic Mach number distribution over the blade surface. The numerical results agree very well with the experimental data.

The first harmonic amplitude and phase angle of the unsteady pressure coefficient are plotted in Figs. 4 and 5 for the cases with IBPA = 90 and 180 deg, respectively. The trends of the computational and experimental data match reasonably well. However, the calculation predicts much higher amplitudes over the front half-chord, a phenomenon that was already mentioned in Ref. 7. The discrepancies in phase are small, which gives the good prediction of the stability range shown in Fig. 6, although the amplitude of the damping coefficient is large compared with the experimental data in the stable region. In the region of instability, much better agreement is achieved. For the investigation of mistuning effects, the test case with $\beta_1 = -10$ deg was chosen, because it is unstable over a slightly larger IBPA range (Fig. 6).

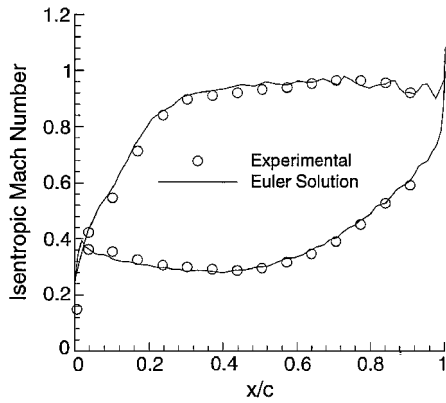


Fig. 3 Steady-state isentropic Mach number distribution over the blade.

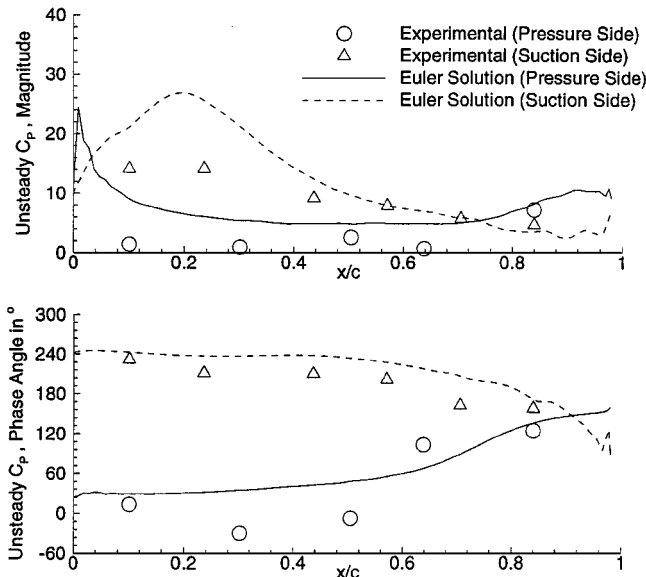


Fig. 4 Amplitude and phase of the first harmonic unsteady pressure coefficient over the blade: IBPA = 90 deg.

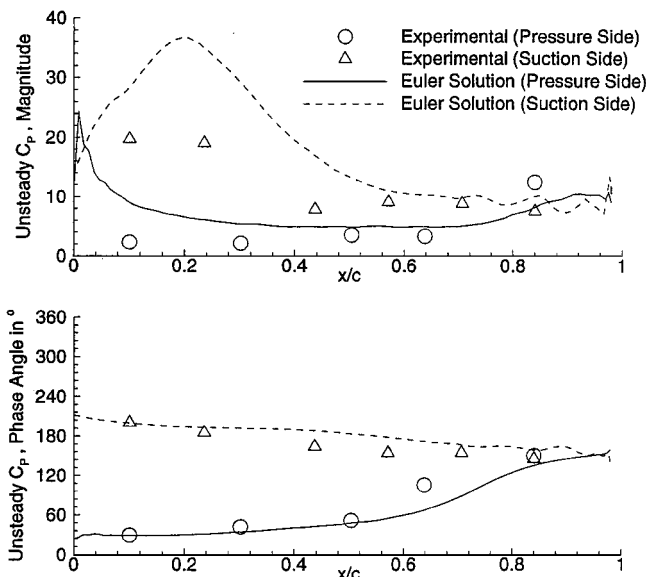


Fig. 5 Amplitude and phase of the first harmonic unsteady pressure coefficient over the blade: IBPA = 180 deg.

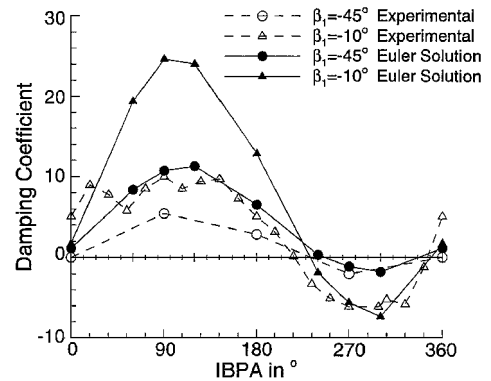


Fig. 6 Damping coefficient over IBPA: $\beta_1 = -45$ and -10 deg.

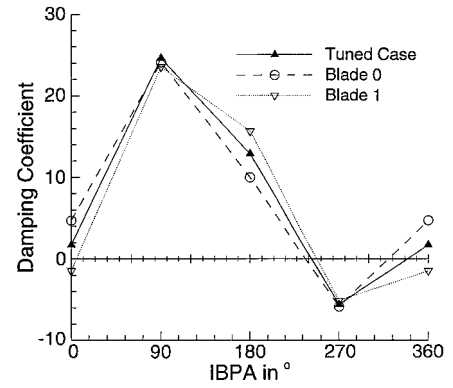


Fig. 7 Damping coefficient vs IBPA for blades 0 and 1. Blade 1 is mistuned in phase by $+10$ deg.

B. Phase Mistuning

In the tuned case, all blades oscillate with identical frequency ω and the same phase difference σ between each pair of adjacent blades as defined by Eq. (11). A simple way of mistuning the system is to slightly change the phase of one of the blades, so that the IBPA is not constant over the blade row. For example, blade 1 in Fig. 2 can be mistuned by a phase shift $\Delta\sigma$, such that

$$\begin{bmatrix} h_x^{(1)}(t) \\ h_y^{(1)}(t) \\ \alpha^{(1)}(t) \end{bmatrix} = a \begin{bmatrix} \mu_x \\ \mu_y \\ \mu_\alpha/c \end{bmatrix} \exp[i(\omega t + \sigma + \Delta\sigma)] \quad (13)$$

The phase difference between blades 0 and 1 then becomes $\sigma + \Delta\sigma$, and $\sigma - \Delta\sigma$ between blades 1 and 2, whereas all other IBPA remain at the original value σ . Although this type of phase mistuning is somewhat artificial, because a real system would pick up its own phase differences based on the flow and structural conditions, it serves the purpose of studying the potential effect of mistuned phase on the motion of flutter.

Figures 7 and 8 show the calculated damping coefficient Ξ as a function of σ for this type of phase mistuning and $\Delta\sigma = +10$ deg. The phase difference σ in this plot is the average IBPA of the cascade, which is the same as in the tuned case. Using only four passages limits the choice for σ to 0, 90, 180, and 270 deg. For these IBPAs, the results for the tuned case, already shown in Fig. 6, are also plotted in Figs. 7 and 8.

It is obvious that, due to mistuning, the damping coefficient Ξ varies for different blades. However, only blades 0 and 1 show significant changes with respect to the tuned case. Mistuning blade 1 affects principally itself and its immediate neighbors, i.e., blades 0 and 2. The blade order is such that blade number $i + 1$ is adjacent to the suction side of blade i (Fig. 2). The flow on the suction surfaces of the blades is more sensitive to changes in conditions than that on the pressure surfaces. Consequently, blades 0 and 1 will be affected most by the mistuned motion of blade 1. The flow around blade 2 is

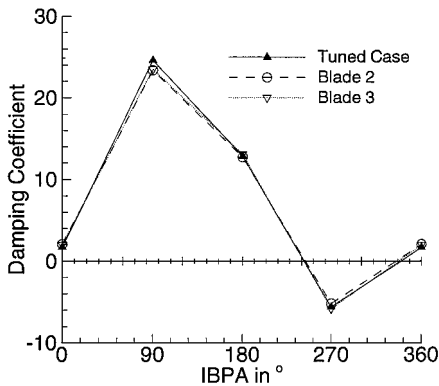


Fig. 8 Damping coefficient vs IBPA for blades 2 and 3. Blade 1 is mistuned in phase by +10 deg.

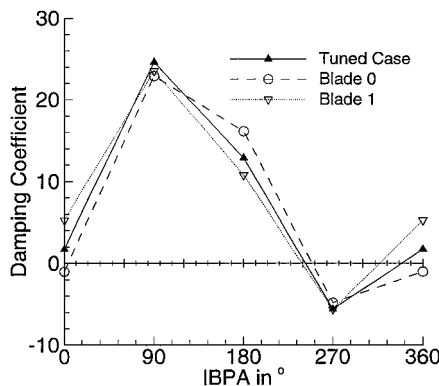


Fig. 9 Damping coefficient vs IBPA for blades 0 and 1. Blade 1 is mistuned in phase by -10 deg.

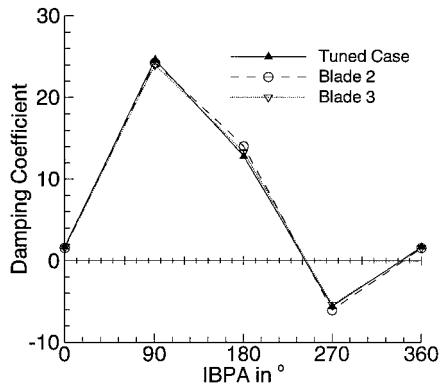


Fig. 10 Damping coefficient vs IBPA for blades 2 and 3. Blade 1 is mistuned in phase by -10 deg.

not affected very much, because it has only its less-sensitive pressure side facing blade 1.

The changes in damping coefficient and therefore stability go in opposite directions for blades 0 and 1, as shown in Figs. 7 and 8. Blade 0 mainly feels a phase difference of $\sigma + 10$ deg at its suction side. At any σ the mistuned value of Ξ qualitatively changes toward the tuned value for $\sigma + 10$ deg. The damping coefficient of blade 1, dominated by a phase difference $\sigma - 10$ deg on the suction side, shifts to the tuned value at $\sigma - 10$ deg. This qualitative behavior also holds for a negative $\Delta\sigma$, as demonstrated by the computational results shown in Figs. 9 and 10. It can be seen that $\Delta\Xi$ is small at relative extrema and large in between. In general, the absolute value and sign of $\Delta\Xi$ appear to depend on the imposed mistuning phase difference $\Delta\sigma$ and the slope of the tuned stability curve. If $\Delta\sigma$ is

considerably small, the effect of phase mistuning can be expressed by the following:

$$\Delta\Xi \sim \left. \frac{\partial\Xi}{\partial\sigma} \right|_{\text{tuned}} \cdot \Delta\sigma$$

C. Frequency Mistuning

Another way to introduce mistuning is to let the blades oscillate with slightly different frequencies. In a first study, this is done again with a single blade of four, i.e., blade 1 in Fig. 2 vibrates with a slightly higher frequency than the other blades. To resolve the small difference $\Delta\omega$ between the tuned and the introduced mistuned frequency, the calculations have to be performed over a longer period of time T than in the tuned case, i.e., $T/T_{\text{tuned}} = \omega/\Delta\omega$.

The motion of the mistuned blade 1 is expressed as

$$\begin{bmatrix} h_x^{(1)}(t) \\ h_y^{(1)}(t) \\ \alpha^{(1)}(t) \end{bmatrix} = a \begin{bmatrix} \mu_x \\ \mu_y \\ \mu_\alpha/c \end{bmatrix} \exp[i(\omega t + \Delta\omega t + \sigma)] \quad (14)$$

For $\Delta\omega = \frac{1}{14}\omega$ the influence on the damping coefficient is shown in Figs. 11 and 12. Again only blades 0 and 1 are significantly affected. The damping of the mistuned blade 1 is independent of the IBPA. This is not surprising, because the concept of a constant IBPA does not apply any more to blade 1. The phase differences of blade 1 with respect to the three other blades are continuously changing in time. After one period of the mistuned system, blade 1 has gone through all IBPAs from 0 to 360 deg. Its damping coefficient is close to the tuned Ξ averaged over the IBPA, which is a positive (stable) value. Blade 0 still has constant IBPAs with respect to blades 2 and 3. The permanently changing phase difference with respect to its suction side neighbor (blade 1), however, weakens the IBPA dependence of blade 0. It becomes stable at any IBPA. Blades 2 and 3 hardly change, compared with the tuned case.

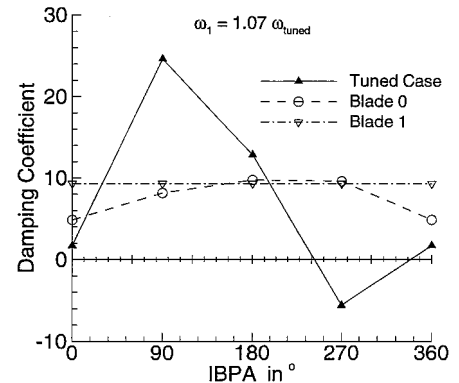


Fig. 11 Damping coefficient vs IBPA for blades 0 and 1. Blade 1 is mistuned in frequency by +7%.

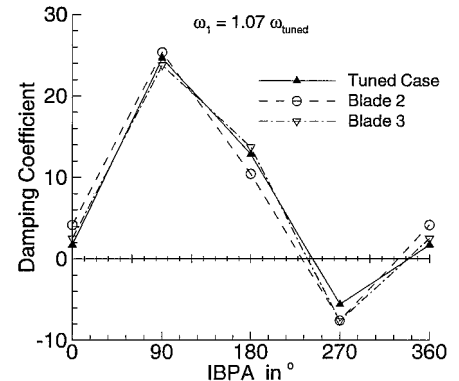


Fig. 12 Damping coefficient vs IBPA for blades 2 and 3. Blade 1 is mistuned in frequency by +7%.

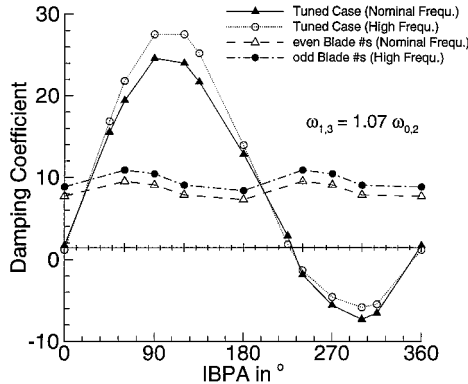


Fig. 13 Damping coefficient vs IBPA. Odd-numbered blades are mistuned in frequency by +7%.

The positive effect on the mistuned blade itself and on one of its neighbors leads to the idea of alternate mistuning: every second blade in the row is mistuned in the same way, i.e.,

$$\begin{bmatrix} h_x^{(m)}(t) \\ h_y^{(m)}(t) \\ \alpha^{(m)}(t) \end{bmatrix} = a \begin{bmatrix} \mu_x \\ \mu_y \\ \mu_\alpha/c \end{bmatrix} \exp[i(\omega t + \Delta\omega t + m\sigma)]$$

$$m = 1, 3, 5, \dots \quad (15)$$

Figure 13 shows the result for the same amount of frequency mistuning as in the previous case, but here it is imposed on blades 1 and 3. In this case, all blades are stable, with little dependence on the IBPA. The reason for this behavior can be explained as follows. Because the frequency of every other blade in the row is perturbed from its nominal frequency, each blade is vibrating at a frequency different than its two immediate neighbors. There is not a fixed IBPA between any blade and its immediate neighbors. If we neglect the influence by far neighbors, each blade can be viewed as the mistuned blade in the single blade mistuning situation discussed earlier and shown in Fig. 11, with either a positive or negative frequency perturbation. Consequently, the damping coefficient for this blade would be independent of the nominal IBPA and would take the phase average of the tuned values. For this case it becomes positive, and therefore the blades become stable. Because this is true for every blade in the row, we expect that all blades become stable with this alternate mistuning pattern. Indeed, this is confirmed by the computational result shown in Fig. 13. The two sets of damping coefficients corresponding to the odd- and even-numbered blades are both positive and almost independent of the nominal IBPA. The slight differences between the two sets are due to the frequency difference between the blades. The two tuned cases shown in Fig. 13 indicate that in the tuned case, the blade motion becomes more stable with increasing frequency at almost all IBPAs. The odd-numbered blades can be viewed as mistuned from its neighbors with a positive frequency perturbation, whereas the even-numbered blades can be viewed as mistuned with a negative frequency perturbation. As such, the phase-averaged damping coefficient for the odd-numbered blades becomes higher than that for the even-numbered blades.

These findings agree qualitatively with the experiment data by Nowinski and Panovsky,⁶ although our computations and analysis were performed independently, for a different cascade and without the knowledge of the experimental results.

Although the effect of far neighbors is small, it is still noticeable in Fig. 13. The damping coefficients are not exactly constant. Instead, they exhibit small variations with the nominal IBPA at twice the frequency as that in the tuned case. This is because there is still a fixed phase difference between each blade and its second neighbors, and that phase difference is exactly twice the nominal IBPA.

The effect of alternate mistuning in this case can be thought of as splitting the blade row into two staggered tuned systems damping each other. The effect of frequency mistuning should not be thought of as an introduction of new damping. It is rather taking away the IBPA-specific influence of neighboring blades. Whether

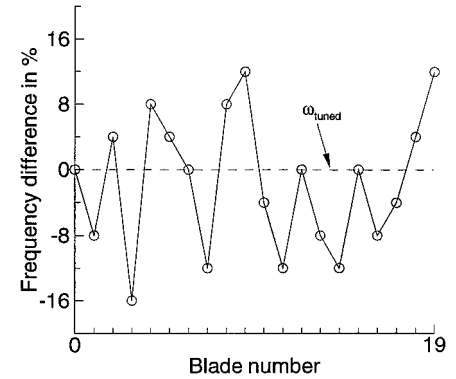


Fig. 14 Randomlike frequency distribution over 20 blades.

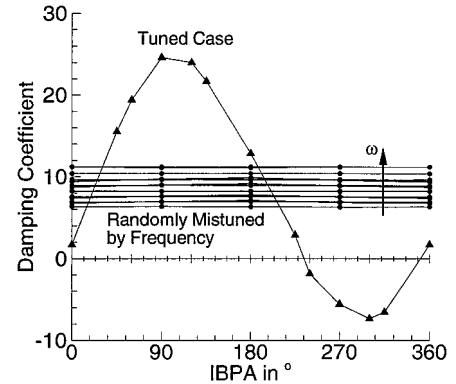


Fig. 15 Damping coefficient for configuration shown in Fig. 14.

this leads to more or less stability than in the tuned case depends on the phase-averaged damping coefficient at the given frequency. It may be expected that this type of mistuning might introduce absolute instability if the tuned blades exhibit instability over most of the IBPA range. We have yet to find such a test case to verify this conjecture.

Aerodynamic decoupling of adjacent blades and, in this case, stabilization is achieved by alternating the frequency. However, there is no need for the frequency to follow a certain pattern throughout the cascade, as long as immediate neighbors oscillate with different frequencies. The effect is expected to be even stronger if we apply a randomlike frequency distribution on a large number of blades (Fig. 14). The damping coefficient for this configuration is shown in Fig. 15. The horizontal lines are the calculated damping coefficients of the individual blades. There is almost no dependence on the IBPA, because blades oscillating at the same frequency are too distant to influence each other. It is also evident from Fig. 15 that the higher the frequency, the larger is the damping coefficient, as in the case in Fig. 13.

It is clear from this discussion that frequency mistuning may stabilize a blade row. The question arises as to how much mistuning, i.e., $\Delta\omega$, is needed. Even if $\Delta\omega$ is infinitesimally small, the phase difference between adjacent blades would still be constantly changing with time, although at a slower rate. The damping coefficient is defined as

$$\Xi = -\frac{C_W}{\pi h^2}, \quad C_W = \frac{T_{\text{tuned}}}{T} \int_0^T C_h dh \quad (16)$$

where T_{tuned} is the period of the tuned case. Our computations show that the beneficial effect of frequency mistuning is not affected by the frequency difference $\Delta\omega$ if one looks only at the damping coefficient defined by Eq. (16). This obviously cannot be true when $\Delta\omega$ goes to zero in the limit of the unstable tuned case. To understand this situation, we must recognize that the damping coefficient as calculated from Eq. (16) in an uncoupled energy method is only a measure of stability over the overall period T . In the case of frequency mistuning, the overall period T is different from T_{tuned} because the blades are oscillating with different frequencies. The

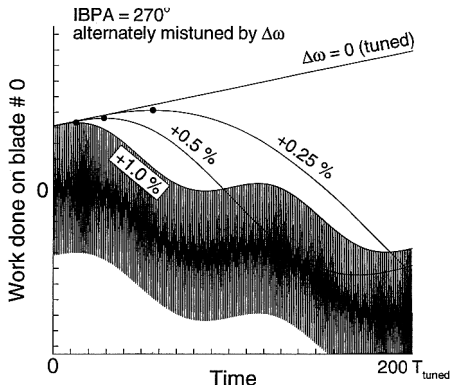


Fig. 16 Work done on blade 0 vs time for various frequency differences.

overall period is determined by the smallest frequency difference that appears in the system. With decreasingly small frequency differences $\Delta\omega$, the overall period becomes very long and the phase differences between adjacent blades change very slowly. It is conceivable that an originally unstable blade may absorb a large amount of energy from the flow during an initial period of time when the phase-angle differences between blades have not yet changed much from the initial nominal value, although the total energy absorption will eventually become negative over the long overall period T . In that case, the damping coefficient calculated by Eq. (16) would not be meaningful, because the blade may already have broken before time T is reached.

To verify this point, we perform calculations of the alternate mistuning case, with $\Delta\omega = 1.0, 0.5, 0.25$, and 0% (tuned case) at the most critical IBPA of 270 deg. Figure 16 shows the instantaneous work coefficient done on blade 0 vs time for the different mistuning cases. For clarity, only the envelope, i.e., the temporal maximum of work, is plotted, except for the case when $\Delta\omega = 1.0\%$. All cases start off with amplification. The total maximum is reached at about the first quarter period, and its magnitude increases continuously with decreasing frequency difference. This maximum may exceed the allowable deformation work, and the blade will break, although the theoretical damping coefficient by Eq. (16) is still a positive number. Short of using a coupled fluid structure interaction approach, such as that described by He,¹³ it is not possible to obtain a quantitative measure of the needed $\Delta\omega$, except the qualitative guidance.

IV. Conclusions

A computational method for predicting flutter of turbomachinery cascades with mistuned blades is presented. The method is based on solving the unsteady Euler/Navier-Stokes equations through multiple blade passages on a parallel computer. Each individual blade is capable of moving with its own independent frequency and phase angle, therefore allowing flutter predictions with either frequency or phase mistuning. Computations for a turbine blade row show that mistuning in phase has relatively small effect on the flutter characteristics of the blade row. On the other hand, frequency mistuning can have significant influence on the damping coefficient of the mistuned blade and its adjacent neighbor. The result is a damping coefficient averaged over the complete IBPA range (0 – 360 deg), because the actual phase differences between the mistuned blade and its adjacent blades are constantly changing within that range, due to the frequency difference. If the blade is stable over most of the IBPA range in the tuned case, the blade will then become stable in an overall sense in the mistuned case. When this effect is made use of

in constructing a blade row with alternately or randomly mistuned blades, it is found that frequency mistuning may stabilize all blades over the whole effective IBPA range. Random mistuning eliminates entirely the dependence of the aerodynamic damping on the IBPA. The minimum amount of mistuning needed for stability is also investigated. It is identified that a blade may absorb too much energy from the flow if there is not enough frequency difference, such that it may fail in a short time, although the overall aerodynamic damping is positive over a long period. The studies in this paper, however, are limited to the use of the energy method, which is only valid for blades with large mass ratios. More definite studies that include the effect of frequency and phase shift of the structural system and accurate prediction of the blade vibration amplitude must be performed with a coupled fluid structure interaction method.

Acknowledgments

Computations have been performed on the Aeneas parallel computer and the Hewlett-Packard Exemplar SPP2000 parallel computer at the University of California, Irvine. Computations have also been performed on parallel machines provided by the National Partnership for Advanced Computational Infrastructure. The authors would like to thank Stefan Irmisch and Thomas Sommer at Asea Brown Boveri Power Generation, Baden, Switzerland, for useful discussions on the topic of mistuning.

References

- ¹Lane, F., "System Mode Shapes in the Flutter of Compressor Blade Rows," *Journal of the Aeronautical Sciences*, Vol. 23, Jan. 1956, pp. 54–66.
- ²Erdos, J. L., and Alzner, E., "Numerical Solution of Periodic Transonic Flow Through a Fan Stage," NASA CR-2900, 1978.
- ³Kaza, K. R. V., and Kielb, R. E., "Flutter and Response of a Mistuned Cascade in Incompressible Flow," *AIAA Journal*, Vol. 20, No. 8, 1982, pp. 1120–1127.
- ⁴Crawley, E. F., and Hall, K. C., "Optimization and Mechanisms of Mistuning in Cascades," *Journal of Engineering for Gas Turbines and Power*, Vol. 107, No. 2, 1985, pp. 418–426.
- ⁵Imregun, M., and Ewins, D. J., "Aeroelastic Vibration Analysis of Tuned and Mistuned Blade Systems," *Unsteady Aerodynamics of Turbomachines and Propellers Symposium Proceedings*, Cambridge Univ. Press, Cambridge, England, U.K., 1984, pp. 149–161.
- ⁶Nowinski, M., and Panovsky, J., "Flutter Mechanisms in Low Pressure Turbine Blades," American Society of Mechanical Engineers, ASME Paper 98-GT-573, 1998.
- ⁷Bölc, A., and Fransson, T. H., "Aeroelasticity in Turbomachines—Comparison of Theoretical and Experimental Cascade Results," *Communication du Laboratoire de Thermique Appliquée et de Turbomachines*, No. 13, Ecole Polytechnique Fédérale de Lausanne, Lausanne, Switzerland, 1986.
- ⁸Ji, S., and Liu, F., "Flutter Computation of Turbomachinery Cascades Using a Parallel Unsteady Navier-Stokes Code," *AIAA Journal*, Vol. 37, No. 3, 1999, pp. 320–327.
- ⁹Wilcox, D. C., "Reassessment of the Scale-Determining Equation for Advanced Turbulence Models," *AIAA Journal*, Vol. 26, No. 11, 1988, pp. 1299–1310.
- ¹⁰Jameson, A., "Time Dependent Calculations Using Multigrid, with Applications to Unsteady Flows Past Airfoils and Wings," *AIAA Paper 91-1596*, June 1991.
- ¹¹Liu, F., and Ji, S., "Unsteady Flow Calculations with a Multigrid Navier-Stokes Method," *AIAA Journal*, Vol. 34, No. 10, 1996, pp. 2047–2053.
- ¹²Alonso, J. J., and Jameson, A., "Fully-Implicit Time-Marching Aeroelastic Solutions," *AIAA Paper 94-0056*, Jan. 1994.
- ¹³He, L., "2-Dimensional Aero-Structure Coupling in Multi-Bladerow Environment," *VKI Lecture Series, Aeroelasticity in Axial-Flow Turbomachines*, May 1999.

E. Livne
Associate Editor